Environmental Research Letters

LETTER

Implications of a shrinking Great Salt Lake for dust on snow deposition in the Wasatch Mountains, UT, as informed by a source to sink case study from the 13–14 April 2017 dust event

S McKenzie Skiles[1] , Derek V Mallia[2], A Gannet Hallar[2], John C Lin[2] , Andrew Lambert[2], Ross Petersen[2] and Steven Clark[1]

[1] Department of Geography, University of Utah, Salt Lake City, UT, United States of America
[2] Department of Atmospheric Science, University of Utah, Salt Lake City, UT, United States of America

E-mail: m.skiles@geog.utah.edu

Abstract

The deposition of dust on snow accelerates melt by perturbing snow albedo, directly by darkening the snow surface and indirectly by enhancing snow grain growth. The snow darkening process impacts hydrology by shifting runoff timing and magnitude. Dust on snow deposition has been documented in the Wasatch Mountains, snowmelt from which accounts for up to 80% of surface water supply for Salt Lake City, UT, but the impact on snow melt has not yet been investigated. Here, we present a case study of a dust event observed in the Wasatch (13–14th April, 2017), sampled coincidentally in the air and at the snow surface at an instrumented high elevation site (Atwater Study Plot, Alta, UT). Atmospheric backtrajectory modeling, the results of which were supported by measurements, showed that dust originated predominantly from the west: the Great Salt Lake Desert and the Great Salt Lake (GSL) dry lake bed. The deposited dust mass accounted for ~50% of the season total dust loading in snow, and daily mean radiative forcing of 20–50 W m^{-2} accelerated snow melt by approximately 25%. This has important implications for The Greatest Snow on Earth®, and snow water resources; the water level of the GSL has been declining, exposing dry lake beds, and there are no legal water rights or protections to maintain lake levels or mitigate dust emission.

1. Introduction

Wind blown dust has important impacts on human and natural systems. Wind eroded dust has important ecological impacts (Field *et al* 2010), adversely impacts air visibility, air quality and human health, and affects atmospheric processes and radiative forcing (RF) (Tegen *et al* 1996, Miller *et al* 2004, Creamean *et al* 2013, Goudie 2014). Upon deposition, dust can influence chemistry and nutrient availablity, and accelerate snow melt (Ballantyne *et al* 2011, Carling *et al* 2012, Niwano *et al* 2012, Skiles *et al* 2012, Brahney *et al* 2013). Episodic dust events are regularly observed across the Western US, with the number of dust events and emissions peaking during the spring. This timing corresponds to increasing winds and the drying out of

arid and disturbed source regions across the Colorado Plateau and Great Basin (Steenburgh *et al* 2012, Sorooshian *et al* 2013, Flagg *et al* 2014, Skiles and Painter 2016). Although dust source regions are inherently stable due to physical and biological crusts, modern settlement and disturbance of the West reduced threshhold frictional velocities of surface soils, leading to significant increases in dust deposition (Belnap and Gillette 1998, Neff *et al* 2008).

Many Western US dust source regions are upwind of mountain snowpacks that are the 'water towers' of the Western US, providing important water storage for nearby population centers (Bales *et al* 2006). Dust deposition enhances snow melt rates by lowering surface albedo: directly in the visible wavelengths, and indirectly in the near infrared wavelengths by

enhancing snow grain growth (Painter *et al* 2007). Spring time dust deposition is particularly effective at enhancing snow melt because, (1) the timing coincides with increasing solar irradiance and peak snow water equivalent, and (2) the dust is not entrained in melt, such that individual dust layers combine at the surface to compound albedo decay (Skiles and Painter 2017). The dynamics and hydrologic impacts of dust on snow have been well studied in the San Juan Mountains of southwestern, CO where a growing body of literature has demonstrated that dust shifts snowmelt timing and magnitude, reduces total water yield, and introduces errors in snowmelt forecasting (Painter *et al* 2010, Skiles *et al* 2012, Bryant *et al* 2013, Deems *et al* 2013, Skiles *et al* 2015).

The impacts of dust on snow have been less well studied in the Wasatch Mountains, which are located in northern Utah, adjacent to the Great Salt Lake (GSL) and Salt Lake City (SLC). Wind blown dust has been studied along the Wasatch Front (Hahnenberger and Nicoll 2012, Steenburgh *et al* 2012, Reynolds *et al* 2014), and impacts on air quality and air visibility are recognized; yet no study has been published to date that has investigated the radiative impacts of deposited dust, or constrained the impact on snowmelt in the Wasatch Mountains. Like other mountains in the Western US, the Wasatch snowpack is a critical natural reservoir, providing up to 80% of surface water resources to the city of Salt Lake (Bardsley *et al* 2013). Notably, snowmelt runoff for the municipality of Salt Lake comes from four watersheds along the Wasatch Front with limited storage along the streams, which makes accurate forecasting of snowmelt timing and magnitude critical for effective management of snow water resources. Additionally, snow plays an important role in the local economy, the Wasatch Mountains are a winter sport destination with 10 ski resorts within one hour of the SLC airport, allowing access to what the State of Utah has officially claimed as The Greatest Snow on Earth®. Accelerated melt and 'dirty snow' could impact this critical sector, the economic impact of which is over a billion dollar annually ($1.15 billion in '15-'16, $1.43 billion in '16-'17; (Leaver 2018).

The objectives of this paper are to characterize a dust event from 13–14th April, 2017 through emission, transport, and deposition and ensuing radiative impact on snowmelt. This event was sampled in transport and at the snow surface at an alpine snow study plot, and then atmospheric backtrajectory modeling was used to investigate the emission and transport of dust. Although dust impacts on snow chemistry have been assessed in the Wasatch (Carling *et al* 2012), and the properties of deposited dust explored (Reynolds *et al* 2014), this is the first study to target a single dust event and assess the life cycle of the dust from source to sink, and to quantify the radiative impact of deposited dust. This particular event was targeted for more detailed study because the source regions were

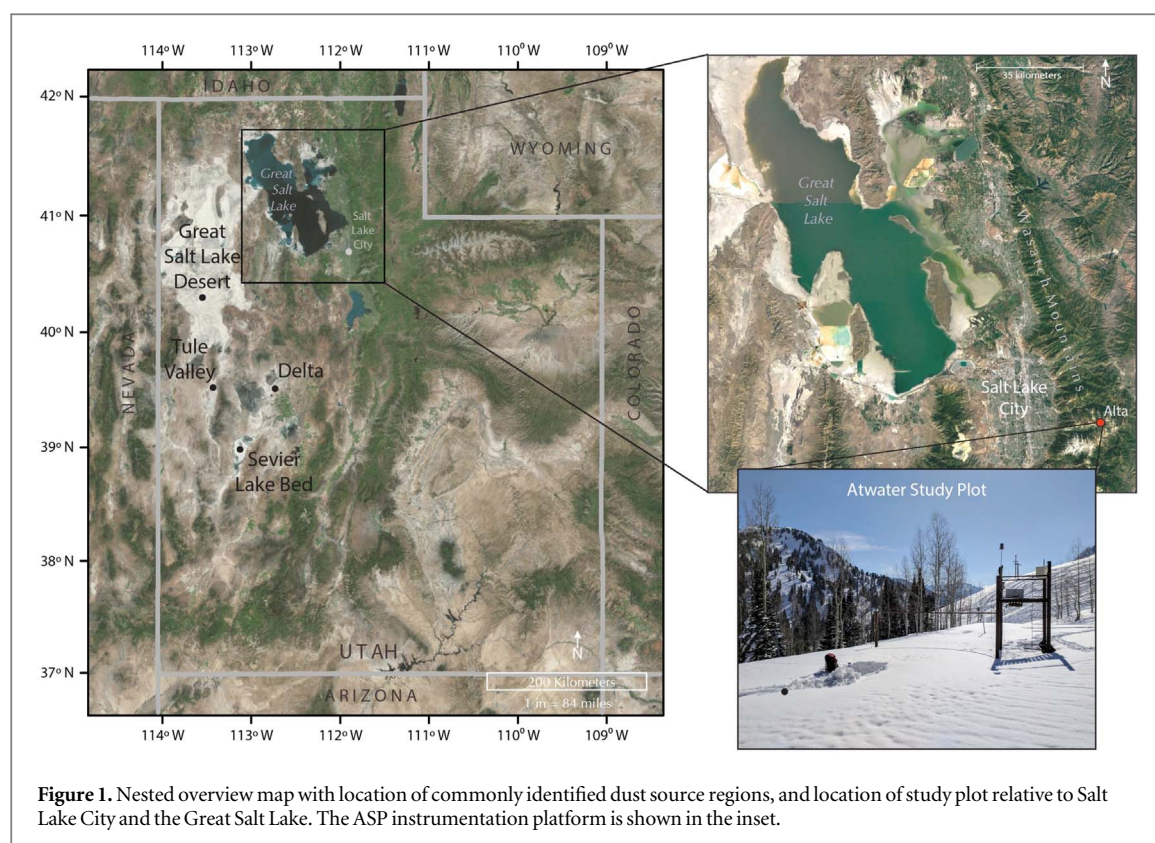identified as being located to the west of the Wasatch, which included the dry lake bed of the GSL.

The GSL is of interest because it has been in steady decline since settlement of the Salt Lake Valley, with lake area dwindling by ~50%, due to upstream water withdrawals (Wurtsbaugh *et al* 2017). There are currently no legal water rights to maintain lake levels of the GSL, and we hypothesize that as the dry lake bed of the GSL expands with increasing populations/water demand, dust events that originate from the dry lake bed will increase in frequency. For example, the planned but currently delayed Bear River Development project (Utah Division of Natural Resources 2017) would divert water from the GSL's primary tributary and expose an estimated additional 80 km^2 of dry lake bed (Wurtsbaugh *et al* 2017). The 13–14th April, 2017 dust event gives us insight to the dynamics of these dust events and how they could impact the adjacent mountain snowpack in the future.

2. Methods

2.1. Study plot

The aerosol and snow measurements presented here were collected at Atwater Study Plot (ASP), Little Cottonwood Canyon, UT, which is located ~18 miles south east of SLC, UT (40.591206° N, 111.637685° W; figure 1). The United States Forest Service established the site in 1939 for snow and avalanche research, and it is currently maintained by the Utah Department of Transportation. The relatively flat plot is about ¼ acre in size (~1000 m^2), at an elevation of 2667 m, and is in an opening in the aspen and conifer forest. A 3 m platform is located in the eastern third of study plot where data collection and instrumentation equipment is mounted, including an aerosol sampler (GRIMM portable aerosol spectrometer, described further below). During this study temperature and relative humidity (Vaisala™ hmp45c) were measured on the main platform, and snow depth (Campbell Scientific™ SR50A) was measured off of a master stake to the west of the main platform. Wind speed and direction were not measured, but due to the protection from the trees, which are ~20–30 m from the platform on all sides, wind speeds are low at the site.

Long term snow depth records from the NRCS snow observation network show that Water Year 2017 (1 October, 2016–31 September, 2017) was an above average snow year for the Wasatch, for example, snow depth at the Alta snow course was 124% of average in April. At ASP snow depth peaked in early March 2017 at 289 cm. A general pattern of high pressure and clear skies during March led to a steady decline in snow depth, but snowfall through April and the beginning of May maintained snow depths around 200 cm. After the first week in May snow melt initiated again and snow depletion occurred on 30th May. There were five visually observed episodic dust events coincident with

Figure 1. Nested overview map with location of commonly identified dust source regions, and location of study plot relative to Salt Lake City and the Great Salt Lake. The ASP instrumentation platform is shown in the inset.

snow cover during Spring 2017; three in March (3/5, 3/23, and 3/31), and two in April (4/7, 4/13). The full dataset will be published elsewhere. Here, we primarily focus on the 13th April event, which was of interest because it is potential source region and because deposited the most dust mass. The other events visually, as observed from the Salt Lake Valley, originated predominantly from the south and were relatively minor in terms of deposited dust mass. Snow pits were excavated to observe snow properties and sample dust concentrations following the event (14th April), and two additional times prior to snow depletion. We note that in local time (MST) the event occurred on 13th April, but in UTC time it spanned the 13th–14th.

2.2. Aerosol sampling

A Portable Aerosol Spectrometer (hereafter GRIMM) manufactured by Grimm Aerosol Technik GmbH & Co. KG, Ainring, Germany (Model 1.109) sampled from 12 to 29 April, 2017 and again from 11 to 31 May, 2017 at ASP. The data gap was due to communication and software issues with the instrumentation. The GRIMM is an optical particle counter that uses a 655 nm laser with a sample flow rate of $1.2\,l\,min^{-1}$ ($\pm5\%$ constantly through control). The particles are detected using scattered light to obtain an aerosol size distribution (for additional details see e.g. Burkart *et al* (2010) and papers cited within). The GRIMM classifies the particles into 31 size channels in the range of 0.25–$32\,\mu m$. The instrument was attached to an aerosol inlet that included 2.54 cm diameter stainless-

steel tube connected to a stainless-steel rain cap with approximately a 10 cm diameter. The GRIMM was attached to the inlet system via a custom made stainless-steel pickoff. To improve aerosol transmission through the inlet, an external pump was attached to the system. The pump pulled at approximately $7.2\,l\,min^{-1}$. The calculated transmission shows a 50% cut-off at approximately $7\,\mu m$ for this inlet system.

2.3. Aerosol modeling

In an effort to quantify the impacts of wind-blown dust events along the Wasatch Front for the mid-April dust event, we used a backward Lagrangian modeling framework that was recently developed specifically for dust simulations (Mallia *et al* 2017). This model was able to successfully capture the timing and magnitude of two major dust events across northern Utah during the spring of 2010, when compared to a number of air quality stations along the Wasatch Front. To simulate atmospheric transport, the Stochastic Time-Inverted Lagrangian transport model (STILT), which is a backward Lagrangian Particle Dispersion model, was used to trace the origins of air for ASP (Lin *et al* 2003). Here, STILT backward trajectories were used to link upwind dust source regions to concentration changes of dust at our region of interest (ASP). The simulations also incorporated a dry deposition scheme that depends upon aerosol size and the land cover (Zhang *et al* 2001). The dry deposition was carried out along each STILT backward trajectory, forward in time at 2 min time increments, identical to methodology described in (Mallia *et al* 2017). Dry deposition was calculated as

a mass survival rate, which also includes gravitational settling. To calculate wet deposition, the GEOS-Chem wet scavenging scheme for soluble tracers was used (Liu *et al* 2001) with dust being assumed to be hydrophilic.

Backward trajectories generated from STILT were driven by wind fields generated from the Weather Research and Forecast (WRF) model at 12 and 4 km resolution (Skamarock *et al* 2008), with the domain centered on the Salt Lake Valley. The North American Mesoscale model was used as boundary conditions for the WRF simulations. Dust emissions (in terms of $PM_{2.5}$ and PM_{10}) for the 13–14 April 2017 event were generated using the FENGSHA dust emission model (Fu *et al* 2014, Huang *et al* 2015, Dong *et al* 2016). In addition to providing STILT with wind fields to drive the air parcel trajectories, WRF also provided friction velocities, land cover, soil type, and soil moisture data to the FENGSHA dust emission model, which runs offline from WRF.

Several modifications were made to the default version of the FENGSHA model so that dust can be emitted from dry lake beds (playa) (Mallia *et al* 2017), which is a major source of dust across the eastern Great Basin (Hahnenberger and Nicoll 2012, Steenburgh *et al* 2012). These changes included adding a new soil type category within the FENGSHA dust emission model, with its own unique friction velocity threshold. A final update was applied to WRF, which included matching the GSL water levels within WRF to GSL levels. Using bathymetry data from the USGS, lake levels within WRF were lowered by 50 cm so that they matched GSL water levels from the spring of 2017. Newly exposed lake bed was then converted from water to playa within WRF.

2.4. Snow observation, sampling, and analysis

Snow samples were collected in three ways: (1) 'bulk' snow surface samples were collected by sampling a shallow layer (∼2 cm) of snow from the surface over a known area, (2) 3 × 50 ml 'vial' samples were collected at the snow surface and each visible dust layer, and (3) 1 l snow samples (from a standard snow density cutter) were collected continuously every 10 cm along the top meter of snow profile and individually bagged. In each snowpit dust and snow layer stratigraphy was noted, snow temperature measured every 10 cm, and snow density/snow water equivalent was measured continuously with the 1 l density cutter. To reduce scavenging of impurities by the sample container, all snow samples were kept frozen after collection and stored in a cold room at −20 °C until time of analysis.

After being removed from the freezer snow samples were allowed to melt completely before recording total sample mass. The 1 l samples were vacuum filtered through individual pre-weighed 0.495 μm Nuclepore pore diameter filters, which were fully

dried and then reweighed to return impurity mass. The large majority of this mass was mineral dust and dust concentration was recorded in micrograms of impurity per gram of snow sample (μg g^{-1} or parts per million by weight). Bulk snow samples were placed in an ultrasonic bath for 20 min to break apart conglomerates, and then particle size distributions were analyzed with laser light diffraction (Malvern Mastersizer). Black carbon was analyzed from vial samples with a single particle soot photometer (SP2; Droplet Measurement Technologies) following established methods and protocols (Wendl *et al* 2014). Black carbon concentrations were low (<10 ppb) enough to have a minimal impact on snow RF, and hereafter we focus on dust.

2.5. Dust in snow RF

RF by dust in snow is calculated by taking the difference in absorption between the albedo of snow containing dust and clean snow albedo for the same grain size, simulated with the offline version of the SNow, ICe, and Aerosol Radiation (SNICAR) model (Flanner *et al* 2007). SNICAR computes multiple scattering and reflectance from snow and aerosol mixtures across 470 bands (0.3–5.0 μm) at 10 nm resolution. Snow property inputs include snow effective grain size, snow density, and aerosol mixing ratios including dust in four size bins. We forced the model with measured snow density, measured dust concentration and particle size distribution, and effective snow grain sizes constrained by snow conditions (supplemental table 1 is available online at stacks.iop.org/ERL/13/124031/mmedia). Total clear sky spectral irradiance, direct plus diffuse, was modeled at the same spectral resolution with the Santa Barbara DISORT Atmospheric Radiative Transfer model (Ricchiazzi *et al* 1998). RF was calculated by taking the summation of the product of spectral irradiance and the difference between the spectrally weighted dust and clean snow albedo from SNICAR, for broadband solar wavelengths:

$$\mathrm{RF} = \sum_{\lambda=0.305\,\mu\mathrm{m}}^{2.5\,\mu\mathrm{m}} I^*(\Delta\alpha)\Delta\lambda, \qquad (1)$$

where I is irradiance and $\Delta\alpha = \alpha_{\mathrm{clean}} - \alpha_{\mathrm{lap}}$ is the difference between clean and dust laden snow albedo at the same hour, for the same snow grain size and density. We refer interested readers to supplemental information for a discussion of uncertainties with this approach.

Total irradiance, albedo, and RF were calculated over the course of the day by varying the solar zenith angle, and daily mean clear sky RF was estimated by integrating across hourly RF values for daylight hours (supplemental figure 1). A simple energy analysis was used to assess the contribution to snowmelt; when the snowpack was fully isothermal (at 0 °C, indicating cold content is depleted and energy is contributing to melt) hourly RF was divided by the enthalpy of fusion
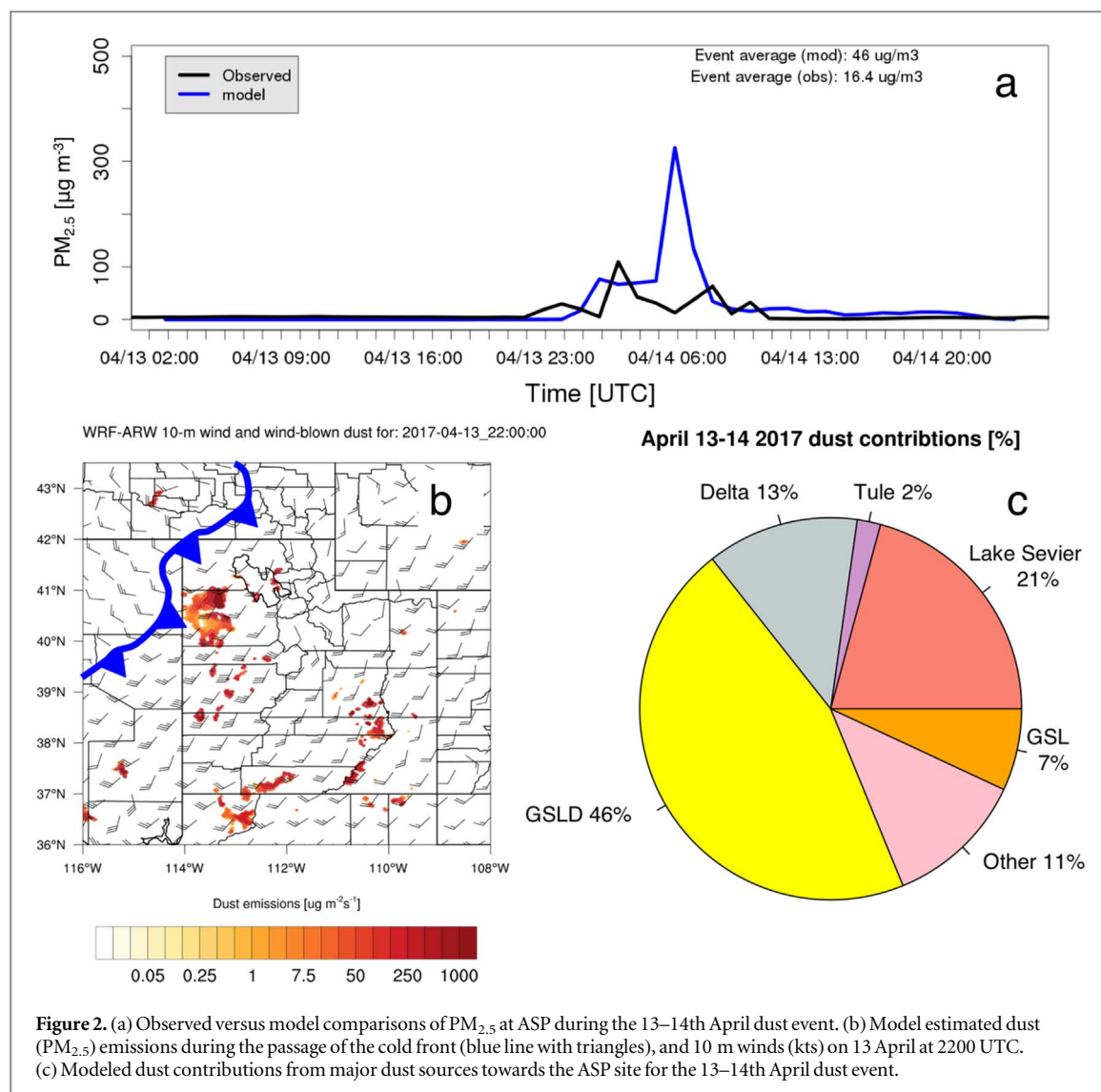
Figure 2. (a) Observed versus model comparisons of PM$_{2.5}$ at ASP during the 13–14th April dust event. (b) Model estimated dust (PM$_{2.5}$) emissions during the passage of the cold front (blue line with triangles), and 10 m winds (kts) on 13 April at 2200 UTC. (c) Modeled dust contributions from major dust sources towards the ASP site for the 13–14th April dust event.

of water at 0 °C (0.334 $\times$ 10^6 J kg^{-1}), to return melt in kg m^{-2}, equivalent to a millimeter of SWE. Melt due to dust RF was compared to SWE depletion, estimated by taking the product of measured snow depths from ASP (continuous), and snow densities from snow pit measurements (discrete) within the period of interest. The intent of this analysis was to get a first order estimate on the magnitude of dust accelerated melt, as we lacked the *in situ* observations to carry out a more thorough snow energy balance modeling approach (Niwano *et al* 2012, Skiles *et al* 2012, Tuzet *et al* 2017).
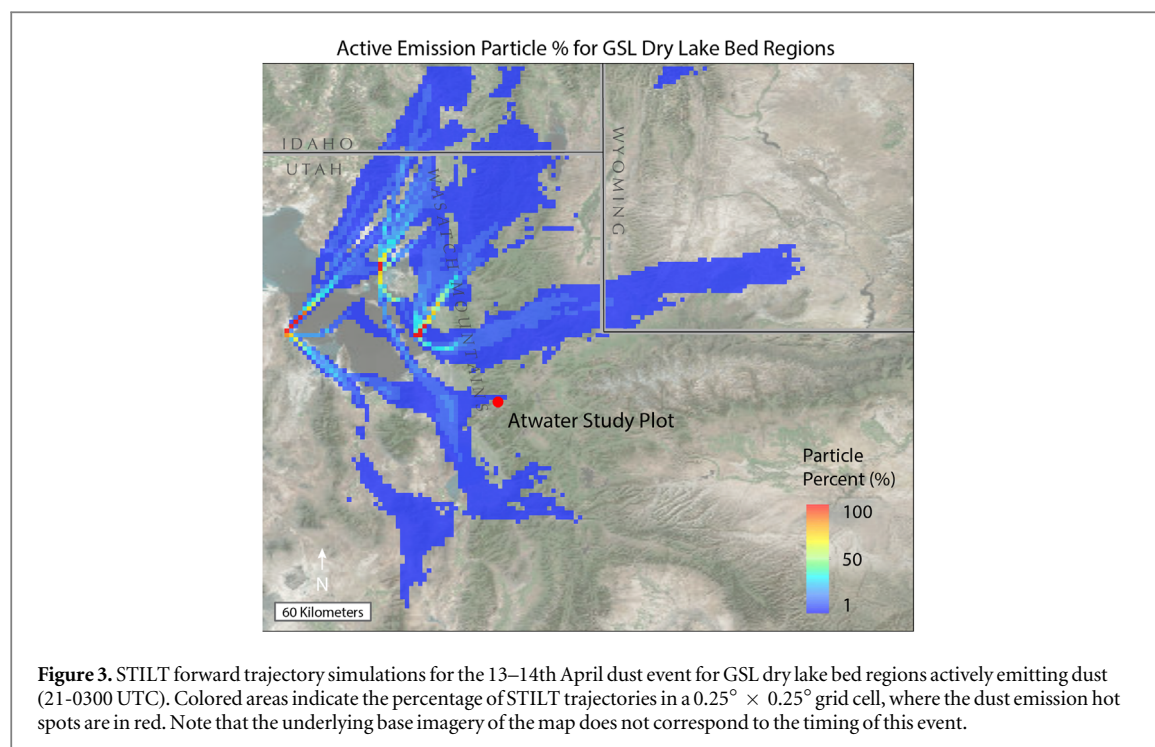
3. Results

3.1. Dust emission and transport
Measured aerosol particle concentrations during the 13–14 April wind-blown dust event (figure 2) started to increase at 0000 UTC, with a sharp increase occurring at 0400 UTC, which was one hour after passage of the cold front (supplemental figures 2–4). This indicates that most of the dust associated with this event was post-frontal. Overall, the WRF-STILT dust

modeling framework was able to capture the timing and duration of the dust event (figure 2(a)). Modeled dust emissions in figure 2(b) indicated that the Great Salt Lake Desert (GSLD), exposed portions of the GSL lake bed, Delta, and Lake Sevier were the largest emitters of dust during this event, which is consistent with results from previous work (Hahnenberger and Nicoll 2012, Steenburgh *et al* 2012, Mallia *et al* 2017). The majority of dust contributions towards ASP, according to WRF-STILT, indicated that the GSLD was the biggest contributor of dust (46%), followed by Lake Sevier (21%), Delta (13%), and other source regions across the eastern Great Basin (11%) (figure 2(c)). The exposed portions of the GSL represented a relatively small fraction of dust contributions towards the ASP site (7%).

Despite ASP seeing limited dust contributions from newly exposed portions of the GSL, model simulations suggest that dry lake bed dust deposited on mountain snow along the Wasatch Mountains. Forward trajectory simulations at dust emission hot spots along the edges of the GSL, which were active between 2100 and 0300 UTC, indicate that the majority of dust

Figure 3. STILT forward trajectory simulations for the 13–14th April dust event for GSL dry lake bed regions actively emitting dust (21-0300 UTC). Colored areas indicate the percentage of STILT trajectories in a 0.25° × 0.25° grid cell, where the dust emission hot spots are in red. Note that the underlying base imagery of the map does not correspond to the timing of this event.

originating from these regions mostly missed ASP, but were transported across the northern Wasatch Mountains (figure 3). Unfortunately, there were no high elevation aerosol measurements in the Northern Wasatch, thus, we were unable to verify dust contributions at these locations.
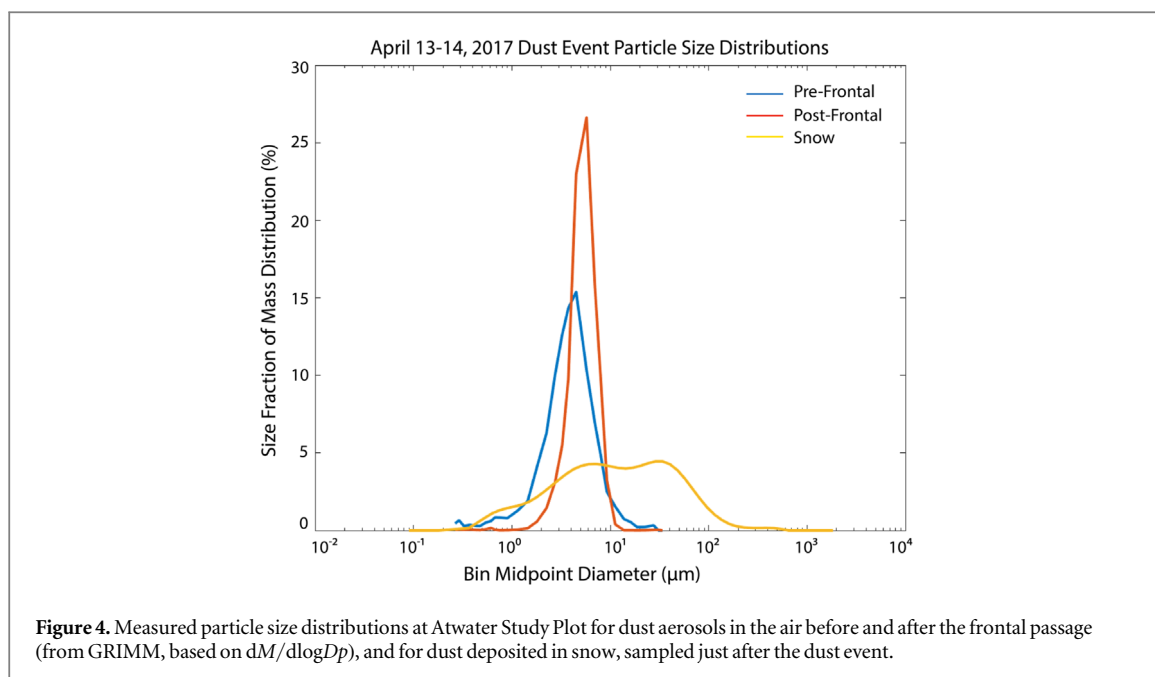
Despite the model being able to capture the timing and duration of the 13–14th April wind-blown dust event, there were significant over estimations in $PM_{2.5}$, by a factor of 3 within the model, relative to those measured at ASP. This could be explained in part by the presence of standing water at dust source regions (supplemental figure 5). MODIS satellite images suggest that portions of the northern GSLD consisted of playa that was saturated with water, or consisted of standing water. The model here is unable to account for temporary standing water, and dust was likely being emitted from grid cells where emissions were unlikely. It is also worth noting that Lake Sevier, which was also a large contributor of dust (21%), had standing water. Other sources of errors within the model include transport errors, as WRF had a delayed frontal passage by upwards of 2 h (supplemental figures 6 and 7).

3.2. Dust deposition and RF

Prior to the dust event the dust concentration at the surface of the snowpack on 10th April was 4 ppm, which increased to 55 ppm on 14th April. The dust from this event was dry deposited and remained exposed at the surface until 20th April, when snowfall buried the dust layer. As a discrete layer 40 cm beneath the surface on 2nd May, the concentration of this layer was 58 ppm, similar to that sampled soon after deposition. This dust layer surfaced on 9th May, and later combined with previously deposited dust layers

on 20th May, just prior to snow depletion on 30th May. At the end of the season, at a proximal but higher elevation site, the concentration of all combined dust layers was 123 ppm. Dust has the tendency to persist in the layer in which it was deposited, and combines at the surface as melt progresses. This process is known as melt amplification (Doherty *et al* 2013). This would indicate that the 14th April dust event accounted for approximately 50% of the total dust mass deposited on snow in water year 2017.

The particle size distribution for deposited dust was bimodal, with peaks at ∼5 and ∼35 μm, with the majority of particles (80%) falling between 2 and 100 μm. We interpret this as indicating dust contribution from multiple sources, one from a more distal source and one from a proximal source. This hypothesis is supported by atmospheric modeling, where prefrontal dust came from areas farther away to the south, while post-frontal passage dust source regions were closer and located to the west of ASP. The further distance over which dust is transported, the more time larger particles have to settle out of the atmosphere via gravitational settling. There was also a shift in peak particle size for aerosols in the air from before and after the frontal passage, with a wider distribution and smaller particles pre-frontal, and a narrower distribution and larger particles after frontal passage, again supporting the model results (figure 4). Deposited particles had a broader size distribution and higher proportion of larger particles relative to those measured in the air. This can be explained by; (1) the GRIMM samples up to 32 μm, and the inlet used for the GRIMM has a low sampling efficiency above 10 μm, (2) the aerosols being sampled by the GRIMM are those that remain in transport whereas the larger particles are

Figure 4. Measured particle size distributions at Atwater Study Plot for dust aerosols in the air before and after the frontal passage (from GRIMM, based on dM/dlogDp), and for dust deposited in snow, sampled just after the dust event.

being deposited, and (3) particle conglomerates that form in the snow are not fully broken apart by the ultrasonic bath prior to particle size analysis. At this point we have no comparison datasets against which to assess these results. Previous work shown a similar shift in particle size for black carbon particles deposited in snow (Schwarz *et al* 2013), but there are no other studies of that we are aware of that coincidentally measure particle size distributions in the snow and in the air for the same dust event.

Just after the dust event on 15th April, the maximum RF by the deposited dust was 33 W m^{-2}, with a daily mean RF of 18 W m^{-2}. During the following clear sky days the daily mean RF increased by $\sim$1 W m^{-2}, due to increasing solar irradiance, and was 23 W m^{-2} on 20th April. The melt due to RF would have been 2–3 mm of SWE per day, and the estimated SWE depletion, $\sim$7–12 mm d^{-1}, indicates dust accounted for $\sim$30% of melt. The dust layer was buried by new snow, and when exposed again on 9th May, the maximum/daily RF was 50 W m^{-2}/26 W m^{-2}, and melt contribution was 4 mm. The RF increased by $\sim$1 W m^{-2} per day through 20th May, and for an average SWE depletion of $\sim$16 mm per day, approximately 25% could be attributed to dust RF. On 20th May, multiple dust layers combined at the surface, bringing the maximum/daily RF up to 95 W m^{-2}/50 W m^{-2}, and melt contribution to 7 mm. Approximately half of the dust, and therefore resulting impact, can be attributed to the 13–14th April dust event. Under the assumption that dust stayed at the surface through snow depletion on 30th May, the maximum/mean daily RF prior to snow depletion would have been 101 W m^{-2}/53 W m^{-2}, which would have contributed 9 mm of melt.
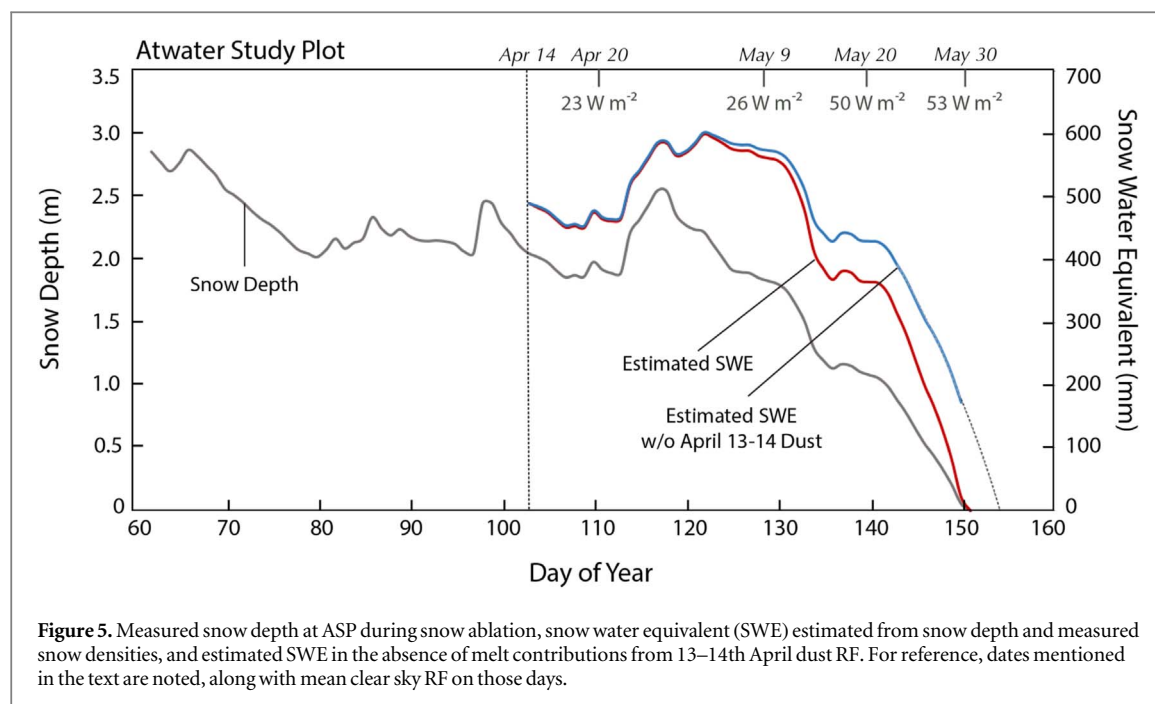
If the SWE loss due to dust from this event is accounted for, a simple SWE depletion forecast indicates the snowpack could have melted out approximately 5 days later in the absence of the mid-April dust event (figure 5). This does not account for total RF by all deposited dust, and also disregards albedo decay feedbacks, like the additional energy from dust accelerating snow grain growth, and therefore the impact is likely greater.

4. Conclusions

We focused on the mid-April dust event because it was a notable event in terms of deposited dust mass and because dust emissions were dominated by source regions to the west of the Wasatch, including the GSL dry lake bed. Although the modeling results indicate that ASP was too far south to be strongly impacted by GSL dust emissions, dust from this event accounted for $\sim$50% of season total dust loading and accelerated melt by $\sim$5 d. The magnitude of dust loading, and radiative impact, was potentially greater for the northern Wasatch (which extends up to the UT/ID border), and therefore, these simulations indicate that a shrinking GSL could impact the Wasatch Mountain's snowpack in the future.

As previously mentioned the majority of dust on snow research has taken place in the San Juan Mountains, the first high elevation point of contact for episodic dust events originating out of the southern Colorado Plateau (Painter *et al* 2007, Skiles *et al* 2012, Bryant *et al* 2013, Skiles and Painter 2017, Painter *et al* 2018). There, high dust concentrations (end of season values range from 1 to 4 mg g^{-1} (pptw)) advance melt by 3–7 weeks, and instantaneous RF can reach over 400 W m^{-2} in extreme dust years (Skiles *et al* 2012). Remote sensing and spatial variability studies show though, that dust RF declines with distance from the

Figure 5. Measured snow depth at ASP during snow ablation, snow water equivalent (SWE) estimated from snow depth and measured snow densities, and estimated SWE in the absence of melt contributions from 13–14th April dust RF. For reference, dates mentioned in the text are noted, along with mean clear sky RF on those days.

southern Colorado Plateau (Painter *et al* 2012, Skiles *et al* 2015), and previous work indicates elsewhere in the Western US impacts may be more similar to those in the Wasatch than those in the southern Rockies (Sterle *et al* 2013, Doherty *et al* 2016). Studies like this give us insight into the magnitude and variability of regional impacts, a scale at which RF by LAPs remains highly uncertain (Skiles *et al* 2018). Additional years of observation and analysis will allow us to further constrain interannual variability.

To our knowledge, these are the first simultaneous measurements of dust size distribution in the air and snow. The size distributions support the model results, which identified two different source regions for dust, areas to the south ahead of the cold front, which then shifted to the west after frontal passage. This study highlights the utility of this approach in providing model validation of dust source regions. Improving dust emission models to identify disturbed areas, for the purpose of dust mitigation, has the potential to help protect ecosystem dynamics, agricultural production, air quality, and human health.

Acknowledgments

ORCID iDs

S McKenzie Skiles ⓘ https://orcid.org/0000-0002-7726-6355
John C Lin ⓘ https://orcid.org/0000-0003-2794-184X

References

Bales R C, Molotch N P, Painter T H, Dettinger M D, Rice R and Dozier J 2006 Mountain hydrology of the western United States *Water Resour. Res.* **42** W08432

Ballantyne A P, Brahney J, Fernandez D, Lawrence C, Saros J and Neff J C 2011 Biogeochemical response of alpine lakes to a recent increase in dust deposition in the Southwestern, US *Biogeosciences* **8** 2689

Bardsley T, Wood A, Hobbins M, Kirkham T, Briefer L, Niermeyer J and Burian S 2013 Planning for an uncertain future: climate change sensitivity assessment toward adaptation planning for public water supply *Earth Interact.* **17** 1–26

Belnap J and Gillette D 1998 Vulnerability of desert biological soil crusts to wind erosion: the influences of crust development, soil texture, and disturbance *J. Arid Environ.* **39** 133–42

Brahney J, Ballantyne A P, Sievers C and Neff J C 2013 Increasing Ca2+ deposition in the western US: the role of mineral aerosols *Aeolian Res.* **10** 77–87

Bryant A, Painter T H, Deems J and Bender S M 2013 Hydrologic response to dust radiative forcing in snow in the upper colorado river basin *Geophys. Res. Lett.* **40** 3945–49

Burkart J, Steiner G, Reischl G, Moshammer H, Neuberger M and Hitzenberger R 2010 Characterizing the performance of two optical particle counters (Grimm OPC1. 108 and OPC1. 109) under urban aerosol conditions *J. Aerosol Sci.* **41** 953–62

Carling G T, Fernandez D P and Johnson W P 2012 Dust-mediated loading of trace and major elements to wasatch mountain snowpack *Sci. Total Environ.* **432** 65–77

Creamean J M *et al* 2013 Dust and biological aerosols from the Sahara and Asia influence precipitation in the western US *Science* **339** 1572–8

Deems J, Painter T H, Barsugli J, Belnap J and Udall B 2013 Combined impacts of current and future dust deposition and regional warming on Colorado river basin snow dynamics and hydrology *Hydrol. Earth Syst. Sci.* **17** 4401–13

Doherty S J, Grenfell T C, Forsstrom S, Hegg D, Brandt R E and Warren S 2013 Observed vertical redistribution of black carbon and other insoluble light-absorbing particles in melting snow *J. Geophys. Res.: Atmos.* **118** 5553–69

Doherty S J, Hegg D A, Johnson J E, Quinn P K, Schwarz J P, Dang C and Warren S G 2016 Causes of variability in light absorption by particles in snow at sites in Idaho and Utah *J. Geophys. Res.: Atmos.* **121** 4751–68

Dong X, Fu J S, Huang K, Tong D and Zhuang G 2016 Model development of dust emission and heterogeneous chemistry within the community multiscale air quality modeling system and its application over East Asia *Atmos. Chem. Phys.* **16** 8157–80

Field J P *et al* 2010 The ecology of dust *Frontiers Ecol. Environ.* **8** 423–30

Flagg C B, Neff J C, Reynolds R L and Belnap J 2014 Spatial and temporal patterns of dust emissions (2004–2012) in semi-arid landscapes, southeastern Utah, USA *Aeolian Res.* **15** 31–43

Flanner M G, Zender C S, Randerson J T and Rasch P J 2007 Present-day climate forcing and response from black carbon in snow *J. Geophys. Res.* **112** D11202

Fu X, Wang S, Cheng Z, Xing J, Zhao B, Wang J and Hao J 2014 Source, transport and impacts of a heavy dust event in the Yangtze River Delta, China, in 2011 *Atmos. Chem. Phys.* **14** 1239–54

Goudie A S 2014 Desert dust and human health disorders *Environ. Int.* **63** 101–13

Hahnenberger M and Nicoll K 2012 Meteorological characteristics of dust storm events in the eastern Great Basin of Utah, U.S.A *Atmos. Environ.* **60** 601–12

Huang M *et al* 2015 Toward enhanced capability for detecting and predicting dust events in the western United States: the Arizona case study *Atmos. Chem. Phys.* **15** 12595–610

Leaver J 2018 *The State of Utah's Travel and Tourism Industry Rep.* Kem C Gardner Policy Institute, University of Utah (http://gardner.utah.edu/wp-content/uploads/2018TourismReport.pdf)

Lin J C, Gerbig C, Wofsy S C, Andrews A E, Daube B C, Davis K J and Grainger C A 2003 A near-field tool for simulating the upstream influence of atmospheric observations: the stochastic time-inverted lagrangian transport (STILT) model *J. Geophys. Res.: Atmos.* **108** 4496

Liu H, Jacob D J, Bey I and Yantosca R M 2001 Constraints from 210Pb and 7Be on wet deposition and transport in a global three-dimensional chemical tracer model driven by assimilated meteorological fields *J. Geophys. Res.: Atmos.* **106** 12109–28

Mallia D V, Kochanski A, Wu D, Pennell C, Oswald W and Lin J C 2017 Wind-blown dust modeling using a backward-Lagrangian particle dispersion model *J. Appl. Meteorol. Climatol.* **56** 2845–67

Miller R, Tegen I and Perlwitz J 2004 Surface radiative forcing by soil dust aerosols and the hydrologic cycle *J. Geophys. Res.: Atmos.* **109** D04203

Neff J C *et al* 2008 Increasing eolian dust deposition in the western United States linked to human activity *Nat. Geosci.* **1**

Niwano M, Aoki T, Kuchiki K, Hosaka M and Kodama Y 2012 Snow Metamorphism and Albedo Process (SMAP) model for climate studies: Model validation using meteorological and snow impurity data measured at Sapporo, Japan *J. Geophys. Res.: Earth Surf.* **117** F03008

Painter T H *et al* 2007 Impact of disturbed desert soils on duration of mountain snow cover *Geophys. Res. Lett.* **34** L12502

Painter T H, Bryant A and Skiles S M 2012 Radiative forcing by light absorbing impurities in snow from MODIS surface reflectance data *Geophys. Res. Lett.* **39** L17502

Painter T H, Deems J S, Belnap J, Hamlet A F, Landry C C and Udall B 2010 Response of Colorado River runoff to dust radiative forcing in snow *Proc. Natl Acad. Sci.* **107** 17125–30

Painter T H, Skiles S M, Deems J S, Brandt T W and Dozier J 2018 Variation in rising limb of Colorado River snowmelt runoff hydrograph controlled by dust radiative forcing in snow *Geophys. Res. Lett.* **45** 797–808

Reynolds R L *et al* 2014 Composition of dust deposited to snow cover in the Wasatch Range (Utah, USA): controls on radiative properties of snow cover and comparison to some dust-source sediments *Aeolian Res.* **15** 73–90

Ricchiazzi P, Yang S R, Gautier C and Sowle D 1998 SBDART: a research and teaching software tool for plane-parallel radiative transfer in the Earth's atmosphere *Bull. Am. Meteorol. Soc.* **79** 2101–14

Schwarz J, Gao R, Perring A, Spackman J and Fahey D 2013 Black carbon aerosol size in snow *Sci. Rep.* **3** 1356

Skamarock W C, Klemp J B, Dudhia J, Gill D O, Barker D M, Duda M G, Huang X Y, Wang W and Powers J G 2008 A description of the advanced research WRF Version 3 *NCAR technical note* Mesoscale and Microscale Meteorology Division. National Center for Atmospheric Research (Boulder, Colorado)

Skiles S M, Flanner M G, Cook J, Dumont M and Painter T H 2018 Radiative forcing by light absorbing particles in snow *Nat. Clim. Change* **8** 964–71

Skiles S M and Painter T H 2016 A 9-yr record of dust on snow in the Colorado river basin *12th Biennial Conf. of Science and Management on the Colorado Plateau* vol 1(http://doi.org/10.3133/sir20155180)

Skiles S M and Painter T H 2017 Daily evolution in dust and black carbon content, snow grain size, and snow albedo during snowmelt, Rocky mountains, Colorado *J. Glaciol.* **63** 118–32

Skiles S M, Painter T H, Belnap J, Holland L, Reynolds R, Goldstein H L and Lin J C 2015 Regional variability in dust on snow processes and impacts in the upper Colorado River Basin *Hydrol. Process.* **29** 5397–413

Skiles S M, Painter T H, Deems J, Landry C and Bryant A 2012 Dust radiative forcing in snow of the Upper Colorado river basin: part II. Interannual variability in radiative forcing and snowmelt rates *Water Resour. Res.* **48** W07522

Sorooshian S, Shingler T, Harpold A, Feagles C W, Meixner T and Brooks P D 2013 Aerosol and precipitation chemistry in the southwestern United States: spatiotemporal trends and interrelationships *Atmos. Chem. Phys.* **13** 7361–79

Steenburgh W J, Massey J D and Painter T H 2012 Episodic dust events of Utah's Wasatch Front and adjoining region *J. Appl. Meteorol. Climatol.* **51** 1654–69

Sterle K M, McConnell J R, Dozier J, Edwards R and Flanner M 2013 Retention and radiative forcing of black carbon in the Eastern Sierra Nevada snow *Cryosphere* **7** 365–74

Tegen I, Lacis A and Fung I 1996 The influence on climate forcing of mineral aerosols from disturbed soils *Nature* **380** 419–22

Tuzet F *et al* 2017 A multilayer physically based snowpack model simulating direct and indirect radiative impacts of light-absorbing impurities in snow *Cryosphere* **11** 2633

Utah Division of Natural Resources 2017 *Bear River Development Project* Water Resources Department of the Utah Division of Natural Resources (Salt Lake City, UT)

Wendl I A, Menking J A, Farber R, Gysel M, Kaspari S, Laborde M J G and Schwikowski M 2014 Optimized method for black carbon analysis in ice and snow using the single particle soot photometer *Atmos. Meas. Tech. Discuss.* **7** 2667–81

Wurtsbaugh W A *et al* 2017 Decline of the world's saline lakes *Nat. Geosci.* **10** 816

Zhang L, Gong S, Padro J and Barrie L 2001 A size-segregated particle dry deposition scheme for an atmospheric aerosol module *Atmos. Environ.* **35** 549–60